Mol Cell Toxicol (2017) 13:419-431
DOI 10.1007/s13273-017-0046-1

ORIGINAL PAPER

Toxicity of TiO_2 nanoparticles on the NRK52E renal cell line

Xavier Valentini[1], Lara Absil[1], Guy Laurent[1], Alexandre Robbe[2], Sophie Laurent[3,4], Robert Muller[3,4], Alexandre Legrand[2] & Denis Nonclercq[1]

Received: 20 September 2016 / Accepted: 30 January 2017

Abstract Titanium dioxide nanoparticles are widely used in industry to produce a number of products (cosmetics, paints, foods). TiO_2 nanoparticles form aggregates and their toxicity varies in function of their size. In this study, aggregate sizes were determined using dynamic light scattering (DLS). The stability of the suspension was evaluated by turbidimetry and the size by transmission electronic microscopy (TEM).
In the present study the toxicity of TiO_2 nanoparticles was evaluated *in vitro* on rat kidney proximal tubular cells (NRK-52E). Cells were exposed to TiO_2 nanoparticles (20 μg/mL) for 24, 48, 72 and 96 hours. TiO_2 nanoparticles induce the production of reactive oxygen species (ROS). The relative number of mitosis decreased, while an increase of apoptotic cells was noted. The number of S-phase cells evidenced by BrdU immunoreactivity in cultures was significantly reduced by the exposure to the nanoparticles. These results attest to the toxic effect of the TiO_2 nanoparticles on NRK-52E cells.

Keywords: 4-Hydroxynonenal, Nanoparticles, NFκB, Oxidative stress, Proliferation

Introduction

Metal oxide nanoparticles represent an industrially important class of nanomaterials. No scientifically accepted definition exists but in general a nanoparticle is defined as an object with at least one of their three dimensions in the range of 1-100 nm[1]. Currently titanium dioxide (TiO_2) nanoparticles (NPs) are produced abundantly and are widely used because of their high stability, catalytic properties and low cost. TiO_2 NPs are a white, odourless powder and can occur in three different crystallographic structures: rutile, brookite and anatase, the latter being used in this study. Some studies have reported that anatase, the most commercially used form, showed higher activity than the rutile form. These particles are frequently used as a white pigment for paints, paper, toothpaste and plastics. They are also widely incorporated in sunscreens due to their capacity to reflect ultraviolet sunrays, and are used in pharmaceutical excipients. TiO_2 has also been used to manufacture articulating prosthesis (hip and knee implants)[2]. Despite the wide range of applications, there is a lack of information on the impact of NPs on human health. On average, humans are exposed to 1 mg/kg body weight per day. The anarchic use of TiO_2 NPs could become a public health problem. Particle dimension is fundamental to their toxicity and some *in vivo* studies have demonstrated that nanoparticles are able to induce a higher toxicity than microparticles[3]. However, it is relevant to note that TiO_2 NPs have a strong tendency to form aggregates. This last point seems to be critical for modulating their potential toxicity. While the formation of aggregates may reduce the effective surface area, NP aggregates show a greater

Electronic supplementary material The online version of this article (doi: 10.1007/s13273-017-0046-1) contains supplementary material, which is available to authorized users.

[1]Laboratory of Histology, University of Mons, Institute for Health Sciences and Technology, Faculty of Medicine and Pharmacy, 23, Place du Parc, B-7000 Mons, Belgium
[2]Laboratory of Respiratory Physiology and Rehabilitation, University of Mons, Institute for Health Sciences and Technology, Faculty of Medicine and Pharmacy, 23, Place du Parc, B-7000 Mons, Belgium
[3]General, Organic and Biomedical Chemistry NMR and Molecular Imaging Laboratory, University of Mons, Institute for Health sciences and Technology and Biosciences, Faculty of Medicine and Pharmacy, 23, Place du Parc, B-7000 Mons, Belgium
[4]Center for Microscopy and Molecular Imaging (CMMI), 8, Rue Adrienne Bolland, B-6041 Gosselies, Belgium
Correspondence and requests for materials should be addressed to X. Valentini (✉xavier.valentini@umons.ac.be)

surface area than microparticles, even in the agglomerated state[4]. In addition to influencing toxicity, the size of NPs also has an impact on their distribution in the organs. It is confirmed that the smallest particles show the most widespread organ distribution including in the blood, heart, lungs, liver, spleen, kidneys, thymus, brain and reproductive organs[5]. TiO_2 NPs can enter the human body through inhalation (respiratory tract), ingestion (gastrointestinal tract), dermal penetration (skin) and injection (blood circulation). In nanomedicine, intravenous and subcutaneous injections can occur.

Some studies have shown that TiO_2 NP exposure is able to cause damage to various organs such as the lungs, liver, kidneys, spleen and brain[6]. It is reported that TiO_2 NPs can induce a large panel of toxic effects, including inflammation, cytotoxicity and genomic instability in mammals, plants and even in microorganisms[7]. Regarding kidney toxicity, data from the literature are controversial. It was showed that even high doses of intravenously injected TiO_2 NPs have a very low impact on renal function, despite strong accumulation in renal tissue[8]. By contrast, another study demonstrated severe renal dysfunction in treated mice, evidenced by a significant elevation of high serum blood urea nitrogen and creatinine levels[9]. TiO_2 NPs are able to induce nephric inflammation through the production of reactive oxygen species (ROS) such as superoxide anions, singlet oxygen and hydrogen peroxide[10].

After their incorporation into eukaryotic cells, TiO_2 NPs have a great ability to produce ROS, such as hydrogen peroxide and hydroxyl radicals. In response to this oxidative stress, affected cells produce a large panel of antioxidants, including reduced glutathiones (GSH) and various enzymes, such as superoxide dismutase (SOD), catalase (CAT), glutathione peroxidase (GPx) and reductase (GSR). ROS production leads both to cytotoxicity and genotoxicity. These antioxidant molecules scavenge the unwanted oxidants but, if oxidative stress persists, it can create alterations in signal transduction and gene expression (mitogenesis, mutagenesis, and apoptosis). GSH is able to neutralise ROS by giving a reducing equivalent and becoming GSSG (oxidised). GSH can be regenerated from GSSG by the enzyme GSR. After TiO_2 NP exposition, the SOD activity of plasma and the GPx activity of the kidneys were significantly decreased and the malondialdehyde (MDA) levels of the liver and kidneys were significantly increased[11]. MDA plays an important role in oxidative stress through its interaction with deoxyadenosine and deoxyguanosine, and leads to DNA damage.

In the present study, the aim was to determine the toxicity of TiO_2 NPs on the NRK52E cell line, derived from rat renal proximal tubules. This cell model was selected to reproduce in vitro the accumulation of TiO_2 NPs in renal tissue. Moreover, the proximal tubule epithelium is one of the primary targets of nephrotoxic injury *in vivo*[12]. Particle size, size distribution and dispersion were defined. Aggregate sizes were determined using dynamic light scattering (DLS). The stability of suspension was evaluated by turbidimetry and finally, transmission electronic microscopy (TEM) was performed to determine and confirm the aggregate and dissociated nanoparticle sizes. NRK52E cells were exposed to particles with different average diameters. To assess TiO_2 nanoparticle toxicity, apoptotic and mitotic indexes were performed and cell proliferation was measured by incubating cells with 5-bromo-2′-deoxyuridine (BrdU). A study of oxidative stress was conducted using immunofluorescence detection of the nuclear migration of NFκB and detection of 4-HNE.

Results

Characterisation of NPs

Dynamic light scattering (DLS) was used in order to determine the size distribution profile of TiO_2 particles in suspension after application of four different methods of dispersion (bath sonicator 1 run of 90 minutes or 3 runs of 30 minutes, probe sonicator 1 run of 90 minutes or 3 runs of 30 minutes). The size of TiO_2 nanoparticles was also characterised and quantified by electron microscopy after the same methods of dispersion (Supplementary figure data 2). After bath sonication an inefficient separation of particles of TiO_2 was obtained that formed large aggregates, including some of between 50 and 250 nm (Supplementary figure data 2). As illustrated in supplementary figure data 1, 3 times 30 minutes runs of probe sonication produced smaller aggregates. The size of NP aggregates determined by DLS was 52 ± 15 nm. In this last case, the mean size of the nanoparticle aggregates, as evaluated by morphometric analysis of electron microscopic fields, was 34 ± 9 nm ($n = 163$) (Supplementary figure data 2). Moreover, measures of turbidimetry indicated that the suspension of nanoparticles obtained by probe sonication (3 runs of 30 minutes) showed the lowest turbidity values and remained stable for more than 24 hours (Supplementary figure data 1).

Morphologic alterations, mitotic and apoptotic indexes

Tubular renal cells NRK52E were exposed to TiO_2 nanoparticles for 24, 48, 72 and 96 hours. Already after 24 hours of exposure to NPs, the presence of macroscopic aggregates was observed dispersed in the cyto-

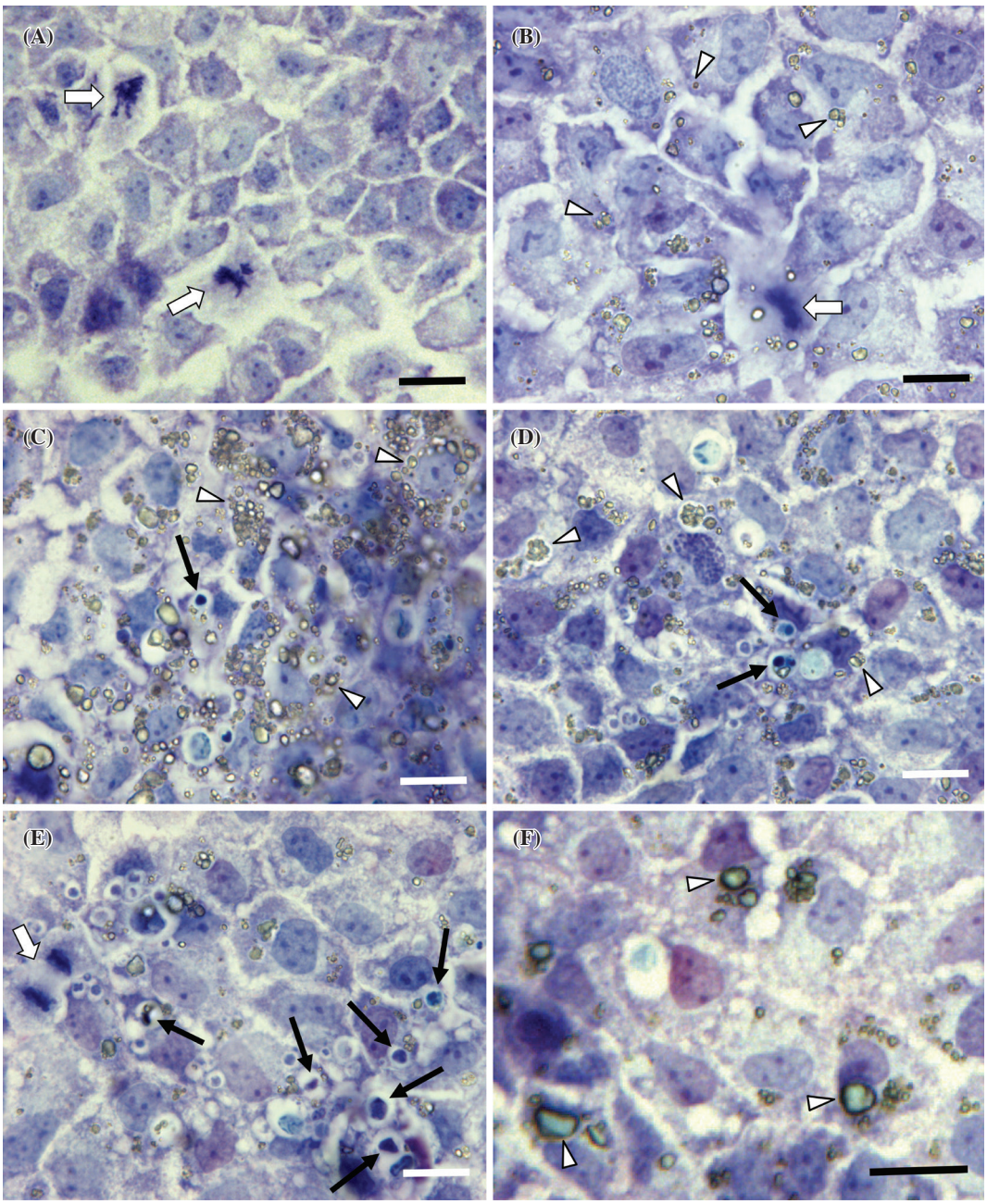

Figure 1. Morphology of NRK52E cells placed in a standard culture medium for 48 hours (control) (A) or exposed to TiO_2 nanoparticles for 24 h (B), 48 h (C), 72 h (D) and 96 h (E, F). These pictures show several mitotic figures (white arrows) that are more frequent in control cells. Apoptotic cells showing picnotic nuclei (black arrows) are present in cultures exposed to nanoparticles and their incidence increased after 72 h and 96 h (D, E). TiO_2 nanoparticles are internalised into phagolysosomes and appeared as spherical refringent inclusions (white arrowheads). The number of TiO_2 inclusions culminated after 48 h (C). After 96 h, the number of aggregates decreased but the size of each intracytoplasmic inclusion increased to reach, in some cases, a diameter of more than 7 μm (F). Scale bars = 15 μm.

plasm of cultured cells (Figure 1). The absence of NPs in the nuclear compartment was also noted. This distribution suggests a sequestration of TiO_2 particles inside the endolysosomal compartment. The number (Figure 2A) and area (Figure 2B) of cytoplasmic aggregates was evaluated by morphometric analysis. A progressive decrease of the number of cytoplasmic aggregates was observed over time accompanied by a concomi-

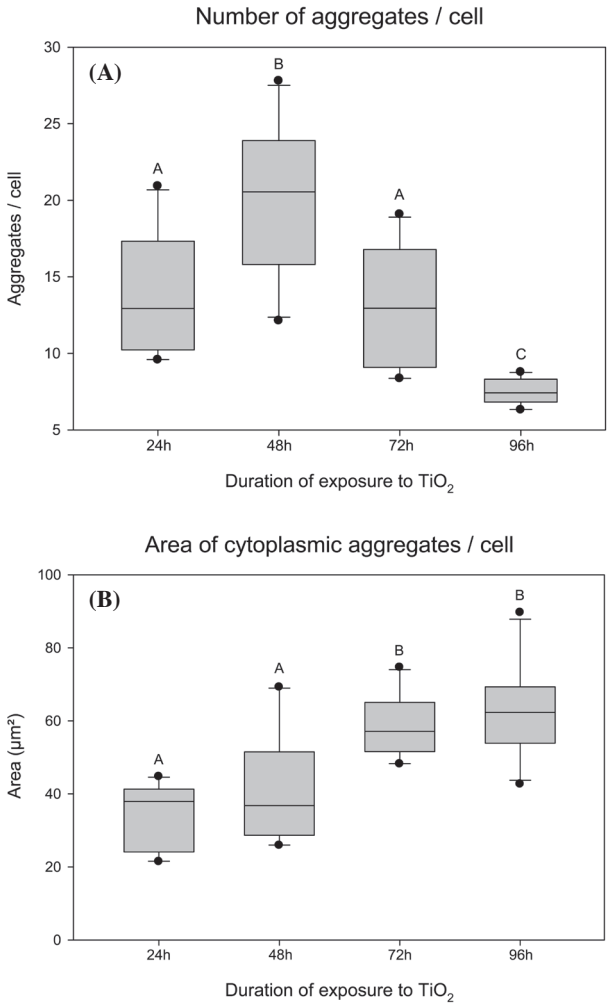

Figure 2. A: Evolution of the number of cytoplasmic TiO_2 aggregates per cell. The number of cytoplasmic aggregates increased to reach a peak at 48 h. After 96 h, a significant decrease of the density of TiO_2 intracytoplasmic inclusions was observed. Letters ((a) versus (b)) indicate significant differences between each experimental time of exposure to TiO_2 ($P<0.05$, Mann-Withney test). B: Morphometric analysis of the area occupied by cytoplasmic TiO_2 inclusions per cell. The cytoplasmic surface of TiO_2 inclusions increased progressively to reach a peak after 96 h. This phenomenon results in a drastic increase of the mean size of TiO_2 inclusions. Letters ((a) versus (b) versus (c)) indicate significant differences ($P<0.05$, Mann-Withney test).

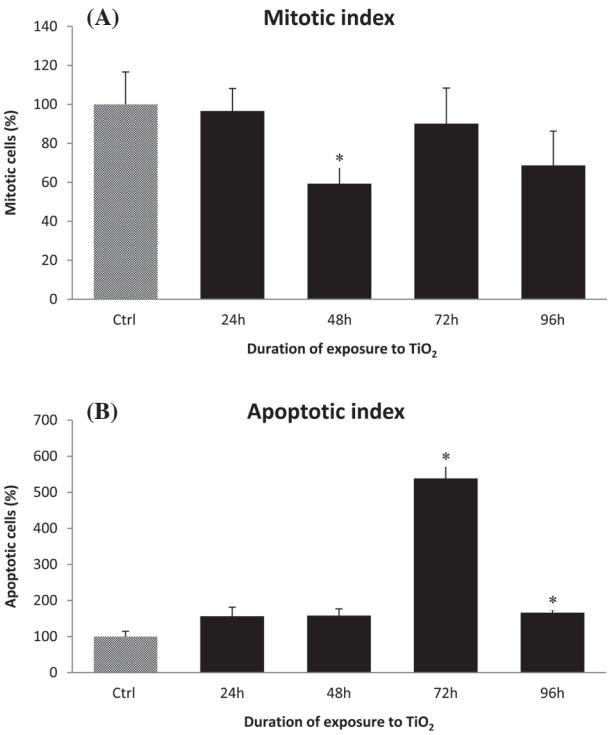

Figure 3. A: Mitotic index after TiO_2 exposure. Values represent the mean percentage of cells in mitosis ± SEM of at least four independent experiments. The percentage of mitotic cells decreased over time with a significant difference between the control and treated cultures at 48 h (*significant values $P<0.05$ versus control cells, Student's t-test). B: Apoptotic index after TiO_2 exposure. Values represent the mean percentage of apoptotic cells ± SEM of at least four independent experiments. Apoptotic nuclei increased over time with a significant difference between the control and treated cultures at 72 h and 96 h (*significant values $P<0.05$ versus control cells, Student's t-test). Control value is normalized at 100%.

tant increase of the aggregate size.

This intracytoplasmic accumulation of TiO_2 has an impact on cell proliferation and viability. On the one hand, as illustrated in Figure 3A, the average number of mitotic cells is lower in cultures exposed to the TiO_2 compared to controls. However, the decline of the mitotic index is only significant after 48 h of culture which is the moment when the cells are undergoing exponential growth phase. On the other hand, the percentage of apoptotic cells was higher in cultures exposed to NPs compared to the control (Figure 3B). Cell death induced by nanoparticle accumulation was not significant during the first 48 hours after exposure to TiO_2 but increased strongly after 72 and 96 hours (Figure 3B).

Cell proliferation evaluated by BrdU incorporation

Proliferating cells were observed in control and treated cultures and are illustrated in Figure 4A and 4B. The immunocytochemical detection of the BrdU incorporated into the DNA allowed the identification of S phase nuclei which had been stained brown. The labelling index, evaluated by morphometry, decreased significantly after 24, 48 hours of exposure to TiO_2 (Figure 4C). In confluent cultures examined at 72 and 96

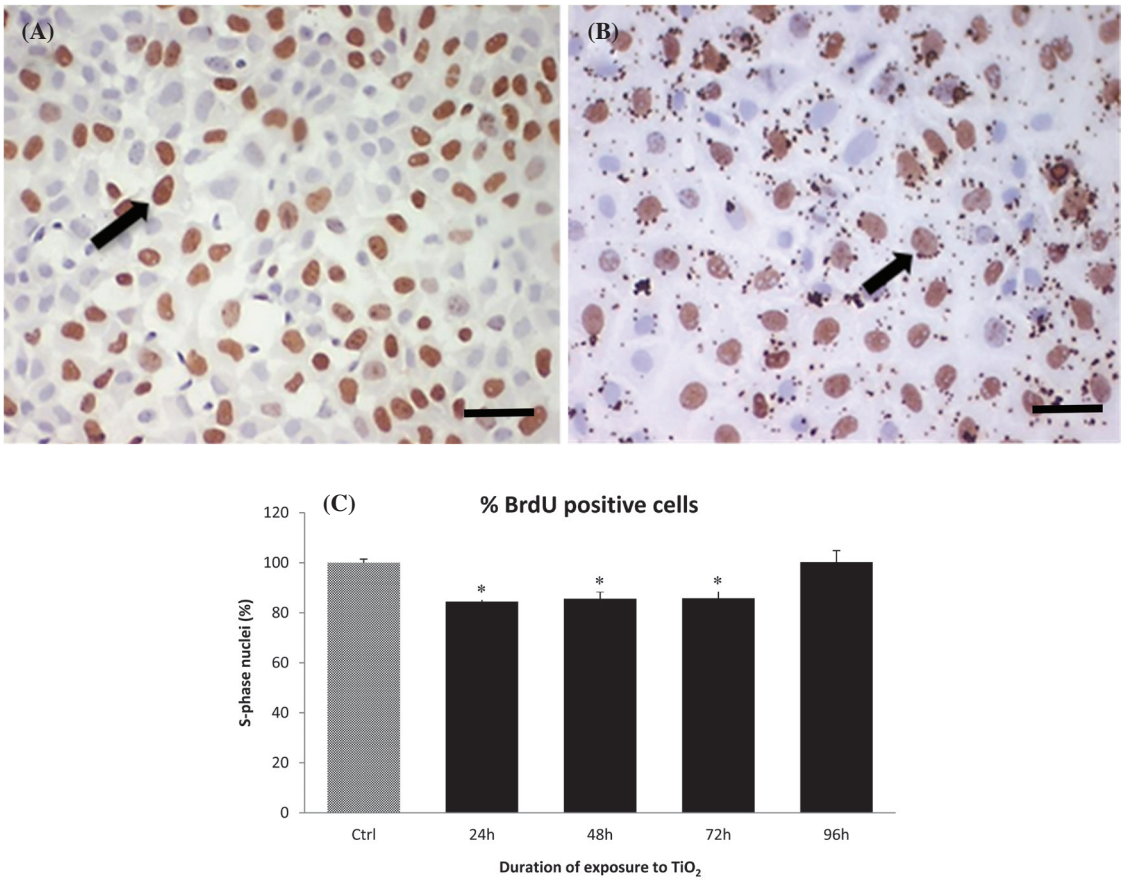

Figure 4. S-phase cells in control culture (A) and after 48 h of exposure to TiO_2 (B). Nuclei of S-phase cells (stained brown) were evidenced by immunocytochemical detection of BrdU (arrows). In the treated culture (B) nanoparticle inclusions appeared as dark spots distributed around nuclei. Scale bars = 25 µm. C: Morphometric analysis of BrdU positive cells. Values represent mean percentage of BrdU positive cells ± SEM of at least four independent experiments. Cell proliferation decreased significantly at 24, 48 and 72 h, compared to control values (*significant values $P < 0.05$ versus control cells, Student's t-test). Control value is normalized at 100%.

hours, no difference of labelling indices was observed between the control and treated cells (Figure 4C).

Detection of oxidative stress

Immunofluorescence labelling of NFκB was used to highlight the production of reactive oxygen species (ROS) and the presence of oxidative stress. The oxidative stress induced a translocation of NFκB from the cytoplasm to the nucleus. The nucleo-cytoplasmic ratio of immunofluorescent signals was analysed and reflected oxidative stress. As illustrated in Figure 5 (A, B), the nuclei of NRK52E cells exposed to TiO_2 were distinctly brighter than the nuclei of control cells. This difference in pattern suggests a nuclear migration of NFκB induced by oxidative stress. The nucleocytoplasmic ratio (N/C) of fluorescence intensity was significantly higher in treated cells at all times of exposure to TiO_2 NPs (Figure 5C).

4-Hydroxynonenal (4-HNE) is an α,β-unsaturated hydroxyalkenal that is produced in large amount by lipid peroxidation in cells exposed to an oxidative stress. 4-HNE was evidenced by immunofluorescence in control and treated cells Figure 6 (A, B). TiO_2-exposed cultures (Figure 6B) present a level of immunofluorescence superior to control cells (Figure 6A). These observations were quantified by morphometric analysis of 4-HNE immunostaining intensities and presented under histogram (Figure 6C).

Discussion

TiO_2 NPs have been considered as inert for a long time and have been used as a "negative control" in many *in vitro* and *in vivo* studies. This was reviewed when an-

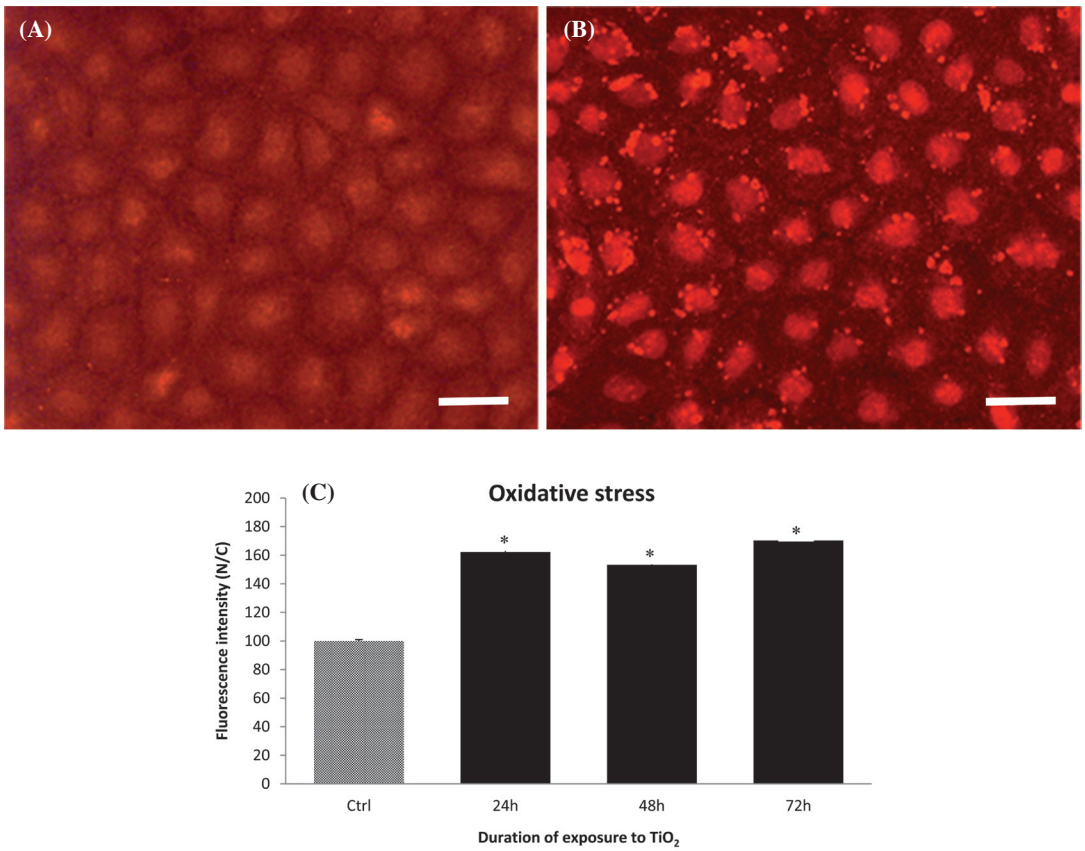

Figure 5. Immunofluorescent labelling of NFκB in control (A) and after 48 h of exposure to TiO_2 (B). Oxidative stress induced a translocation of NFκB immunostaining from the cytoplasm to the nuclear compartment as evidenced in treated cells. Scale bars: 25 µm. C: Quantitative analysis of the nucleo-cytoplasmic ratio of fluorescent signal. Values represent the mean ratio of fluorescence intensity recorded in the nucleus and cytoplasm respectively (N/C) ± SEM of at least four independent experiments. A significant difference was observed in all cultures exposed to TiO_2, compared to control values (*significant values $P<0.05$ versus control cells, Student's t-test). Control value is normalized at 100%.

imals exposed to TiO_2 NPs developed lung tumours[14]. Following this study, TiO_2 NPs were classified as a Group 2B carcinogen.

Anatase and rutile are the two major crystal forms for TiO_2 NPs. The crystalline structure and the surface properties are directly responsible for the differences within their relative toxicity. As demonstrated in many *in vitro* and *in vivo* studies, these two crystal forms are toxic, but the toxicity of anatase is stronger[15,16]. In the present study, it has been shown that TiO_2 NPs (anatase) induced the production of ROS in NRK-52E cells (tubular renal cells) that impacted the cell proliferation rate and could lead to apoptosis. We used an exposition dose of 20 µg/mL. This is an average dose that leads to cell injuries in others studies[17].

Nanoparticles of TiO_2 can get into the blood stream in different ways, such as inhalation and passage across the alveolar cell wall, by ingestion and absorption through gastrointestinal mucosa, or by direct passage through the skin epithelium. The kidneys are an important filtration site and are able to accumulate TiO_2 NPs in different sections of the nephron by absorption or secretion processes[18]. Despite the fact that the kidneys are one of the major target organs for toxicity induced by TiO_2 NPs, very few works have been dedicated to studying their toxicity on various renal cell lines until now. In a recent study, it is showed that the HK-2 cell line derived from kidney proximal tubules is significantly more sensitive than another cell line, IP15, derived from glomerular mesangial cells[19]. They attributed this difference of sensitivity to the highest endocytic capacity of tubular cells. In the present study, another cell line was chosen (NRK-52E) which is also derived from proximal tubules and is commonly used to study pharmacological agents causing renal tubular necrosis[20-23].

The behaviour and activity of NPs is dependent on physical and chemical properties, such as surface area,

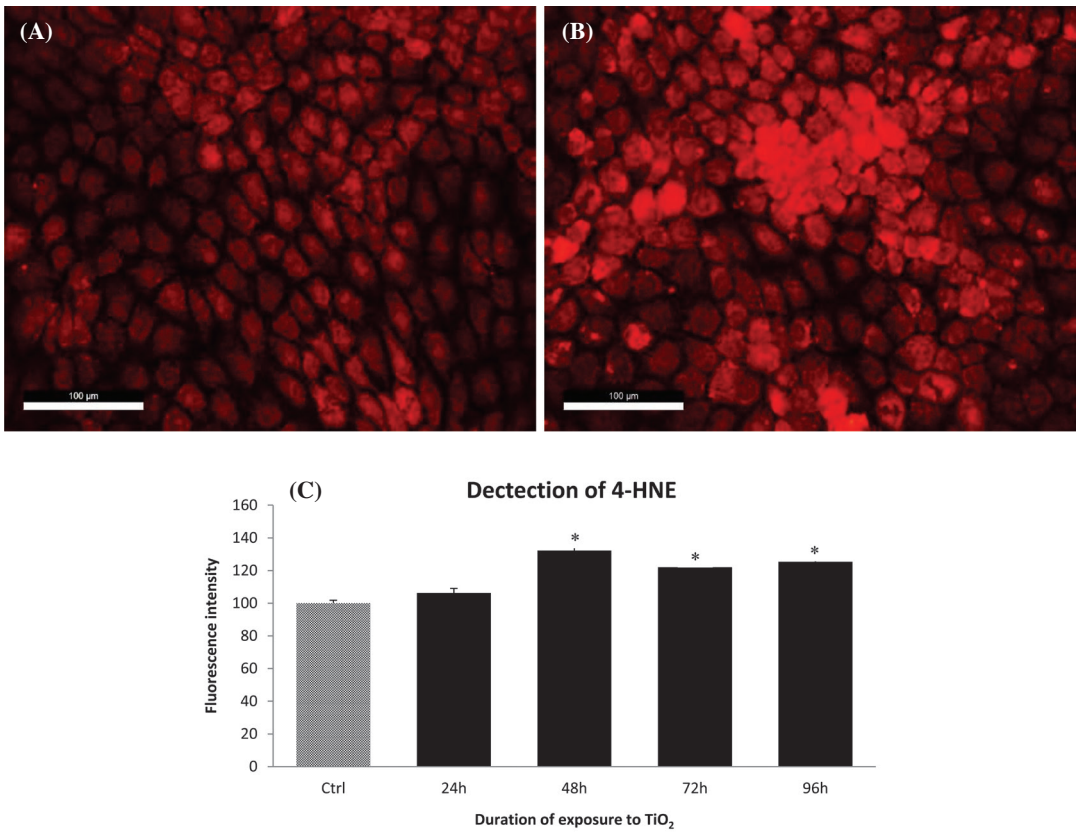

Figure 6. Detection by immunofluorescence of 4-hydroxynonenal (4-HNE) in control (A) and after 96 h of exposure to TiO_2 (B). Oxidative stress induced an increase of fluorescence intensity in TiO_2 treated culture (B) as compared to control (A). Scale bars: 100 µm. C: Quantitative morphometric analysis of fluorescent signal intensities in function of the TiO_2 exposure time. Values represent the mean ratio of fluorescence intensity recorded in cell cultures ± SEM of at least four independent experiments representing at least 10.000 cells/ experimental group. A significant difference was observed in cultures exposed 48, 72, 96 h to TiO_2, compared to control values (*significant values $P < 0.05$ versus control cells, Student's t-test). Control value is normalized at 100%.

aggregation, size distribution. Consequently, a good characterisation of NPs is a crucial step to studying their toxicity and for the understanding and interpretation of results. The major problem encountered in the use of TiO_2 nanoparticles was with obtaining a good dispersion of particles and avoiding the formation of aggregates. The creation of aggregates in solution can be explained by a low anionic charge of the particle surface. Repulsive forces are too low to stabilise suspensions therefore NPs have a strong tendency to form micrometric aggregates. The modification of the size affects the physicochemical characteristics of nanoparticles such as the percentage of surface atoms in contact with the substrate. Consequently, large micrometric aggregates are less reactive than isolated nanometric particles[24,25]. Moreover, particle size is also important for distribution in different organs[26]. This is particularly true for the route of entry by pulmonary inhalation[27]. Smaller particles will penetrate deeper into the respiratory tract: particles of 1-5 nm are mostly distributed in alveolar regions; particles of 20 nm are distributed in the nasopharyngeal region[28]. Small particles can easily penetrate the cells and induce stronger alterations. A study *in vivo* showed that TiO_2 NPs of 20 nm diameter led to a greater pulmonary inflammatory response than NPs with a diameter of 250 nm[29]. The toxicity of TiO_2 NPs on NRK-52E cells was already demonstrated[27]. The cytological observations in TEM performed by Barillet *et al*.[30] clearly shows that NPs are internalized into the cells by micropinocytosis or caveolae-mediated endocytosis and are accumulated in phagolysosomes. This cytological localization of TiO_2 was mentioned in another study[31], performed on keratinocytes, that confirms the uptake of nanoparticles in cells was restricted to phagosomes. Our results corroborate those of Tucci and collaborators[31] which shows an accumulation of nanoparticles in the lysosomal compartment. By contrast, Tucci[31] clams that TiO_2 does not affect cell cycle phase distribution, nor cell death, although our study demonstrates clearly

that exposure to TiO_2 nanoparticle interferes with cell cycle (reduction of S-phase cells and mitotic index) and induces cell apoptosis. These contradictory results are probably due to the fact that the renal tubular cells used in our model have a greater capacity of endocytosis than the keratinocytes and also because we have placed our cell cultures in contact with the nanoparticles over a longer period of time.

In the present study, the use of a probe sonicator allowed the agglomerates to be broken down and the particles to be dispersed more uniformly in the aqueous suspension. This method meant that a mean size of TiO_2 NPs in the nanoscale range of 34 ± 9 nm could be obtained. These ultrafine TiO_2 NPs can be endocytosed and fused with lysosome, which then leads to lysosomal thesaurismosis and the destruction of these organelles. Agglomerates of NPs are shown in the cytoplasm because they are internalised and confined into phagolysosomes where nanoparticles could form macroscopic aggregates. The presence of vesicles full of TiO_2 NPs, probably phagolysosomes, in the cytoplasm of NRK-52E cells can certainly perturb cellular division by preventing the formation of the mitotic spindle and could consequently explain the decrease of the mitotic index evidenced in exposed cultures. This observation was in agreement with a previous study in which the presence of large TiO_2 cytoplasmic vesicles was also observed[32]. They demonstrated that the internalisation of NPs is size-dependent. Indeed, small particles (30 nm) were internalised into the cytoplasm whereas bigger particles (500 nm) remained outside the cells. Disturbing the assembly of mitotic spindle microtubules affects both chromosome segregation and cytokinesis, resulting in aneuploidy, which can lead to cell death or genomic instability. In our study, the impact of TiO_2 on mitotic indexes was only statistically significant after 48 h. 48 h also corresponds to the time interval where the number of intracytoplasmic aggregates of TiO_2 per cell reaches its maximum which could explain that these numerous accumulations could interfere with the establishment of the mitotic spindle. The negative impact observed after 48 h could also be explained by the fact that at 48 h the cells were in the exponential growth phase. This observation is to be related to the significant decrease of S-phase cell number observed after 24 and 48 hours of exposure to nanoparticles of TiO_2. It is possible that the oxidant stress disrupts DNA replication capacity during S phase. The toxic effects of TiO_2 on the number of cells in S phase and mitotic index are less evident when the cells reach confluence after 72 and 96 h. However, at this stage the nanoparticles induce a significant increase in the rate of apoptosis. The increase of apoptosis could results from mitochondrial alterations as evidenced by Tucci and collaborators[31] or from genetic damages highlighted by DNA double strand breaks detected by alkaline comet assay and the immunostaining of γ-H2AX foci[30].

In the present study TiO_2 macroscopic aggregates were not detected inside nucleus. These results suggest that TiO_2 NPs cannot pass massively through the nuclear pores to accumulate inside the nucleus. However, a limited passage of TiO_2 nanometric particles in the nuclear compartment could not be excluded. In this context, it was reported that it is possible for NPs to get into the nucleus under certain conditions[33]. This nuclear distribution is contested in another study[31] attesting that TiO_2 nanoparticles did not enter into the nucleus or any other cytoplasmic organelles except phagolysosomes. When cells are exposed to TiO_2 NPs, there is an increase in the proportion of cells that are stopped in G2/M in a concentration-dependent manner after 24-hour exposure[34]. It is well known that ROS interacts with DNA, disrupts replication and could induce apoptosis. The production of ROS evidenced in this study may explain the decrease in the percentage of BrdU positive cells (S-phase cells) and consequently the increase of apoptotic figures. By contrast, a decrease of apoptotic cells per field after treatment with TiO_2 NPs in a gastric epithelial cell line using the TUNEL method was reported[35]. The study also highlights the production of ROS and the increase of oxidative stress determined by measuring oxidised glutathione (GSSG) in cells treated with 150 μg/mL of TiO_2 NPs compared to controls. Unlike in this present study, the authors noted an increase of proliferation cells[35]. In the aforementioned *in vivo* study, alterations of the balance between cell proliferation and apoptosis may reflect a mechanism of carcinogenesis.

The large surface area of NPs increases their capacity to produce ROS[36]. ROS have been implicated in the activation of transcription factors, such as NFκB, which plays an important role in mRNA transcription coding for antioxidant enzymes. This allows the cell to restore the imbalance between oxidating and antioxidating molecules.

NFκB plays also a role in the activation and phosphorylation of the mitogen activated protein kinase (MAPK) family leading to increased gene transcription. This process results in chromatin remodelling and expression of a range of proinflammatory and antioxidant genes involved in several cellular events, such as cell differentiation, apoptosis and proliferation. ROS production was investigated by nuclear migration of NFκB detected by immunofluorescence[37]. Under action of a stimulus, it is able to migrate to the nucleus. However, it was suggested that the NF-κB is always present in very low concentration in the nucleus, even

if there is no stimulation[38]. The activity of NF-κB is regulated by interaction with inhibitory IκB proteins[39]. The interaction between both proteins blocks the ability of NF-κB to bind to DNA and results in the NF-κB complex being in the cytoplasm. As described in the literature, translocation of NF-κB is an important step in the coupling of extracellular stimuli to the transcriptional activation of specific target genes. NF-κB is activated by pro-inflammatory cytokines (TNF-α, IL-1α), bacterial toxins (exotoxin B), viral products (Herpes Simplex, HIV-1) and cell death stimuli (such as O_2-free radicals, UV light and γ-radiations)[40,41]. In the present study, the ROS produced by the exposure to nanoparticles induced activation of the Nuclear Factor κB (NF-κB) pathway as demonstrated by the translocation of NF-κB protein from the cytoplasm to nucleus. Barillet and collaborators[30] have also evidenced an oxidative stress induced by TiO_2 in NRK52E. In this study, the presence of ROS was evidenced by the increasing fluorescence of 2′,7′-dichlorodihydrofluorescein diacetate acetyl ester. This method is complementary to that used in our study. Another study[19] assessed also that TiO_2 NPs are able to generate ROS in two renal cell lines with a method based on the production of 2′,7′ dichlorofluorescein (DCF). However, no nuclear translocation of NFκB with TiO_2 NPs was reported, whereas it was the case with ZnO and CdS[19]. They noted that cells were able to maintain their antioxidant potential when they were exposed to TiO_2 NPs for 1 hour. In this study, the duration of exposure was longer and could explain the translocation of NFκB in the nuclear compartment. The release of inflammatory mediators from epithelial cells and macrophages was blocked by a mechanism involving the increase of intracellular glutathione and decrease of NFκB activation[42]. 4-HNE has an anti-proliferative effect. Indeed, rapid proliferation is accompanied by low level of lipid peroxidation[43]. This mechanism is partly due to low level of peroxidizable fatty acids in intensively proliferating cells. 4-HNE is able to reduce the proliferative capacity of HL-60 Human promyelocytic leukemia cells and induces the same effect on K562 cell line, derived from a patient with chronic myeloid leukemia[44,45]. The control of apoptosis is affected by ROS and by various products of lipid peroxidation such as 4-HNE. HNE treatment caused glutathione depletion which led to an enhanced apoptosis in PC12 rat phaeochromocytoma cells[46]. This apoptosis is due to an activation of caspases by glutathione depletion. These data are consistent with the results obtained during this study. Indeed, the proliferation of NRK52E cells exposed to TiO_2 nanoparticles decreased over time. A massive apoptosis is also observed in treated cells.

In conclusion, physical characteristics were noted, such as the fact that size of NPs plays a major role in their toxicity. These NPs are already present in the cytoplasmic compartment of the cells after 24 hours of exposure. It has been demonstrated that TiO_2 NPs decrease mitosis and cell proliferation and increase apoptosis. These results show clearly that TiO_2 NPs cause oxidative stress. ROS production and reduced-glutathione (GSH) depletion is probably one of the major causes leading to the apoptotic processes. This study demonstrates that renal tubular cells have a high capacity of capture and internalisation of the titanium oxide nanoparticles. In consequence, this kind of cell could be considered as an important target where the toxicity of this compound is exacerbated. This study means that more can be learnt about the TiO_2 NPs cytotoxicity on renal tubular cells. As perspectives, it would be interesting to explore the nephrotoxicity *in vivo* to well understand the behaviour of NPs in a complex and dynamic system.

Material & Methods

TiO_2 NP preparation

The nanoparticles used in this study were titanium (IV) oxide, anatase with a purity of 99.7%, based on trace of metal analysis obtained from Sigma Aldrich. A stock suspension was prepared in phosphate buffer saline (PBS) (2 mg/mL). Before each application on culture cells, NPs were sonicated in a sonication bath at a frequency of 40 kHz and a power of 600 W (Sonomatic 300) for 15 minutes. All NPs preparation was done under sterile conditions. A volume of 10 µL of nanoparticle stock solution (2 mg/mL) was added per mL of culture medium to obtain a final concentration of 20 µg/mL in contact with treated cells. A volume of 10 µL of vehicle (BPS) was added per mL of culture medium in control cultures. The culture medium was not changed during the incubation periods of 24, 48, 72 and 96 hours.

Cell cultures

All experiments were performed on the established cell line NRK52E (normal rat kidney tubular cells) cultured at 37°C in a cell incubator with humid atmosphere at 5% CO_2 (Nuaire, 5500E). Cells were propagated in 75-cm^2 flasks containing DMEM supplemented with 10% foetal calf serum (FCS), 20 mM N-2-hydroxyethylpiperazine-N′-2-ethanesulfonic acid, 100 U/mL penicillin, 100 µg/mL streptomycin and 0.25 µg/mL amphotericin B. Cells were passed once a week with a renewal of the culture medium 2 days after seeding. For passages, cells were dislodged from the vessel bottom by

trypsin/EDTA. For immunohistochemistry, 12-well plates containing sterile round glass coverslips (12 mm diameter) were seeded with NRK52E cells at a density of 0.5×10^4 cells/cm^2. Concentrations of cells in suspension were measured in a model ZI electronic cell counter (Coulter Electronic, Luton, UK)

Size distribution

Four methods of particle dispersion were tested: i) bath sonicator (sonomatric 300 CeBeCo®, Germany; 600 W) 1 run of 90 minutes, ii) the same protocol but fractioned in 3 runs of 30 minutes, iii) probe sonicator (UP200S, dr.Hielscher Ultrasound technology (GmbH), 50/60 Hz; 230 V) 1 run of 90 minutes, iiii) the same protocol but fractioned in 3 runs of 30 minutes. The average aggregate size of TiO_2 NPs was evaluated by dynamic light scattering (DLS) using a Malvern Zetasizer Nano ZS instrument. DLS is a spectroscopy technique which is used to determine the size distribution profile of small particles in suspension. A laser light is shot through a polariser and then into the sample of particles in suspension. The scattered light then goes through a second polariser where it is collected by a photomultiplier and the resulting image is projected onto a screen. The resulting spectrum is analysed by the Stokes-Einstein equation which provides the hydrodynamic radius of the particles: $R_h = K_B \cdot T/6\pi \cdot \eta_s \cdot D$ (where K_B is the Boltzmann constant, η_s the fluid viscosity and D the diffusion coefficient). NPs were suspended in PBS and dispersed by ultrasound (bath or probe sonicator) as detailed previously. The results obtained with DLS were confirmed using transmission electron microscopy (TEM). A droplet of suspension was deposited on 75 mesh gold Formvar coated grids and air-dried. Nanoparticle aggregates were observed in a Zeiss LEO 906E Electron microscope at 80 kV. Morphometric software (KS400, Zeiss, Germany) was used to determine the size distribution of the nanoparticle aggregates. The stability of aggregates in suspension was evaluated by measure of turbidimetry using a Turbiscan Lab Expert (Formulaction, France).

Evaluation of cell growth and apoptosis

To assess cell growth or apoptosis, the number of mitotic figures or apoptotic nuclei was counted on five microscopic fields, picked at random, per culture slide at 400X magnification. Cell proliferation was also evaluated after the incorporation of BrdU (3 µg/mL culture medium) into the culture medium, 2 hours before cell fixation. BrdU is an analogue of thymidine that can be incorporated into DNA during the S-phase of the cell cycle (DNA replication). BrdU positive cells were detected by immunohistochemistry using a monoclonal anti-BrdU antibody (Dako, Glostrup, Denmark). The procedure was applied to cell cultures after fixation in paraformaldehyde 4% for 15 minutes as detailed in a previous publication[13]. Briefly, culture slices were treated for 30 minutes with a 3 M HCl solution at 60°C. After rinsing, culture cells were preincubated for 20 minutes in a 0.01% caseine solution in PBS buffer. Thereafter, cells were incubated for 1 hour in the presence of mouse monoclonal anti-BrdU antibodies (1 : 20) at room temperature. This was followed by a 30-minute exposure to anti-mouse/peroxidase complexes (ImmPress™ Reagent Kit; Vector, Burlingame, CA). Bound peroxidase activity was visualized by incubation in the presence of 3.3′-diaminobenzidine (DAB) and 0.02% H_2O_2 in PBS. Finally cell preparation were counterstained with Mayer's hemalun and mounted in permanent medium. The number of S-phase cells was counted on 5 microscopic fields picked at random per slide at high magnification 400X representing a total scanned surface of 105,000 µm^2 and approximately 2,500 cells per culture. Measures were done on 4 independent cultures corresponding to a total of approximately 10.000 cells. For each time point, 4 no-treated cultures were analyzed following a similar procedure and were used as controls. For each time point, the mean was calculated on four independent cultures and data presented as histogram ± SEM. Equivalent procedures were done to evaluate the mitotic index as also the number of apoptotic cells.

Evaluation of intracytoplasmic NPs aggregates

For each culture, the number of cytoplasmic aggregates per cell as also the area occupied by nanoparticle aggregates per cell was quantified by morphometric analysis at high magnification (400x). The procedure utilized a hardware consisting of a Zeiss Axioplan microscope equipped with a ProgRest®-C10plus colour camera connected to an IBM PC, and a software designed for morphometry and colour analysis (KS 400 Imaging system, Carl Zeiss Vision GmbH, München, Germany). This image analysing system was able to discriminate intracytoplasmic inclusions of TiO_2 on the basis of difference of colour and contrast. For each culture, 5 microscopic fields were picked at random representing a total scanned surface of 105,000 µm^2 and approximately 2,500 cells. The number of TiO_2 inclusions was quantified and the surface occupied by intracytoplasmic aggregates of TiO_2 per cell was calculated. For each time point, measures were done on 4 independent cultures corresponding to a total of approximately 10.000 cells scanned. Results were presented under box plots.

Detection of ROS production

To investigate the occurrence of oxidative stress, nuclear migration of NFκB was detected by immunofluorescence using a rabbit polyclonal anti-NFκB antibody (Abcam, Cambridge, UK). Cells were permeabilised in PBS containing 0.1% Triton-X-100 three times for 5 minutes and were incubated in blocking solution (casein 0.05%) for 15 minutes to avoid false-positives. Primary antibodies (anti-NFκB) were diluted at 1 : 50 in PBS/casein 0.05%. Incubation with the primary antibody was performed for 1 hour, followed by three washes in PBS/Triton 0.1%, for 5 minutes each. This was followed by a 30-minute exposure to anti-rabbit/peroxidase complexes (ImmPress™ Reagent Kit; Vector, Burlingame, CA), a rabbit anti-peroxidase (1 : 200 in PBS/casein 0.1%) and an anti-rabbit biotinylated antibody (1 : 50 in PBS/casein 0.1%, Dako, Glostrup, Denmark). Cells were rinsed three times for 5 minutes between each antibody. Finally, the preparations were incubated in the fluorescent dye Texas Red/Streptavidin (1 : 50 in PBS, Vector Laboratories, Burlingame) for 30 minutes, rinsed again in PBS and distilled water for 5 minutes, and mounted in Vectashield mounting medium with Dapi (Vector Laboratories, Burlingame). The intensity of fluorescence was measured with the software ImageJ (a public domain image software developed by Rasband W. at the Research Service Branch of the National Institute of Mental Health, NIH). Results expressed the average of nucleocytoplasmic report (N/C) of fluorescence intensity. The nucleocytoplasmic report (N/C) was performed on 5 microscopic fields picked at random per slide at high magnification 400X representing a total scanned surface of 105,000 μm^2 and approximately 2,500 cells per culture. Measures were done on 4 independent cultures corresponding to a total of approximately 10.000 cells. For each time point, 4 no-treated cultures were analyzed following a similar procedure and were used as controls. For each time point, the mean was calculated on four independent cultures and data presented as histogram ± SEM. A second method using a rabbit polyclonal 4-Hydroxynonenal antibody diluted at 1 : 75 (Abcam, Cambridge, UK) was used to highlight an oxidative stress by immunofluorescence following the method described above for NFκB. The 4-Hydroxynonenal is a marker of lipid peroxidation. The intensity of the fluorescent signal recorded in the different groups was evaluated using image processing software (KS 400 imaging system, Carl Zeiss vision, Hallbergmoos, Germany) Measures of immunofluorescence intensity were done on 4 independent cultures corresponding to a total of approximately 10.000 cells. For each time point, 4 no-treated cultures were analyzed following a similar procedure and were used as controls. For each time point, the mean was calculated on four independent cultures and data presented as histogram ± SEM.

Statistical analysis

To study the number of S-phase cells, the mitotic index, the number of apoptotic cells and the ROS production, each of these parameters were performed on 4 independent cultures for each time point. For each time point, 4 no-treated cultures were analysed following a similar procedure and were used as controls. Results are expressed as means ± SEM of four independent cultures and presented as histogram. Comparison of the means between cultures exposed to TiO_2 and control cells (normalized at 100%) was performed using Student's t-test. For all experiments, P values < 0.05 were considered as significant.

The morphometric analysis of the number of intracytoplasmic TiO_2 inclusions per cell as well as the area occupied by these inclusions per cell was also performed on 4 independent cultures for each time point. In this case, the distribution of data is not Gaussian and a no-parametric test (Mann-Whitney) was used in order to compare the experimental data in function of time exposure, P values < 0.05 were considered as significant.

Abbreviations

4-HNE: 4-Hydroxynonenal
BrdU: 5-bromo-2′-deoxyuridine
CAT: catalase
DAB: 3.3′-diaminobenzidine
DCF: 2′,7′ dichlorofluorescein
DLS: dynamic light scattering
GPx: glutathione peroxidase
GSH: reduced glutathiones
GSR: glutathione reductase
GSSG: oxidised glutathiones
MDA: malondialdehyde
NFκB: nuclear factor kappa B
NPs: nanoparticles
ROS: reactive oxygen species
SOD: superoxide dismutase
TEM: transmission electronic microscopy

Acknowledgements The authors thank Mrs. Sylvie Montante for her support in the preparation of NPs. The proofreading by Mrs. Natalie Dickson is gratefully acknowledged. Guy Laurent is Senior Research Associates of the National Fund for Scientific Research (Belgium) and the recipient of a grant from the Belgian Fund for Medical Scientific Research. Sophie Laurent and RNM thank the COST action TD1402, the ARC Programs of the French

Community of Belgium, the UIAP VII programs of Belgium, the FNRS (*Fond National de la Recherche Scientifique*) and the Center for Microscopy and Molecular Imaging (CMMI, supported by the European Regional Development fund and the Walloon Region).

Conflict of Interest Xavier Valentini, Lara Absil, Guy Laurent, Alexandre Robbe, Sophie Laurent, Robert Muller, Alexandre Legrand & Denis Nonclercq declare that they have no conflict of interest.

Human and animals rights The article does not contain any studies with human and animal and this study was performed following institutional and national guidelines.

References

1. Riu, J., Maroto, A. & Rius, F. X. Nanosensors in environmental analysis. *Talanta* **69**:288-301 (2006).
2. Shi, H., Magaye, R., Castranova, V. & Zhao, J. Titanium dioxide nanoparticles: a review of current toxicological data. *Part Fibre Toxicol* **10**:15 (2013).
3. Wang, J. *et al*. Acute toxicity and biodistribution of different sized titanium dioxide particles in mice after oral administration. *Toxicol Lett* **168**:176-185 (2007).
4. Oberdorster, G., Oberdorster, E. & Oberdorster, J. Nanotoxicology: an emerging discipline evolving from studies of ultrafine particles. *Environ Health Perspect* **113**:823-839 (2005).
5. De Jong, W. H. & Borm, P. J. Drug delivery and nanoparticles: applications and hazards. *Int J Nanomedicine* **3**:133-149 (2008).
6. Yu, Y., Ren, W. & Ren, B. Nanosize titanium dioxide cause neuronal apoptosis: a potential linkage between nanoparticle exposure and neural disorder. *Neurol Res* **30**:1115-1120 (2008).
7. Warheit, D. B., Webb, T. R., Reed, K. L., Frerichs, S. & Sayes, C. M. Pulmonary toxicity study in rats with three forms of ultrafine-TiO_2 particles: differential responses related to surface properties. *Toxicology* **230**:90-104 (2007).
8. Scown, T. M. *et al*. High doses of intravenously administered titanium dioxide nanoparticles accumulate in the kidneys of rainbow trout but with no observable impairment of renal function. *Toxicol Sci* **109**:372-380 (2009).
9. Wang, J. J., Sanderson, B. J. & Wang, H. Cyto- and genotoxicity of ultrafine TiO_2 particles in cultured human lymphoblastoid cells. *Mutat Res* **628**:99-106 (2007).
10. Zhao, J. *et al*. Titanium dioxide (TiO_2) nanoparticles induce JB6 cell apoptosis through activation of the caspase-8/Bid and mitochondrial pathways. *J Toxicol Environ Health A* **72**:1141-1149 (2009).
11. Liang, G. *et al*. Influence of different sizes of titanium dioxide nanoparticles on hepatic and renal functions in rats with correlation to oxidative stress. *J Toxicol Environ Health A* **72**:740-745 (2009).
12. Prozialeck, W. C., Edwards, J. R., Lamar, P. C. & Smith, C. S. Epithelial barrier characteristics and expression of cell adhesion molecules in proximal tubule-derived cell lines commonly used for in vitro toxicity studies. *Toxicol In Vitro* **20**:942-953 (2006).
13. Brohée, R. *et al*. Demonstration of estrogen receptors and of estrogen responsiveness in the HKT-1097 cell line derived from diethylstilbestrol-induced kidney tumors. *In Vitro Cell Dev Biol Anim* **10**:640-649 (2000).
14. Lee, K. P., Trochimowicz, H. J. & Reinhardt, C. F. Pulmonary response of rats exposed to titanium dioxide (TiO_2) by inhalation for two years. *Toxicol Appl Pharmacol* **79**:179-192 (1985).
15. Sayes, C. M. *et al*. Correlating nanoscale titania structure with toxicity: a cytotoxicity and inflammatory response study with human dermal fibroblasts and human lung epithelial cells. *Toxicol Sci* **92**:174-185 (2006).
16. Jin, C. Y., Zhu, B. S., Wang, X. F. & Lu, Q. H. Cytotoxicity of titanium dioxide nanoparticles in mouse fibroblast cells. *Chem Res Toxicol* **21**:1871-1877 (2008).
17. Chen, Z. *et al*. Genotoxic evaluation of titanium dioxide nanoparticles in vivo and in vitro. *Toxicol Lett* **226**: 314-319 (2014).
18. Wang, J. *et al*. Acute toxicity and biodistribution of different sized titanium dioxide particles in mice after oral administration. *Toxicol Lett* **168**:176-185 (2007).
19. Pujalté, I. *et al*. Cytotoxicity and stress induced by different metallic nanoparticles on human kidney cells. *Part Fibre Toxicol* **8**:10 (2011).
20. Piron, A. *et al*. In vitro demonstration of a mitogenic activity in renal tissue extracts during regenerative hyperplasia. *Am J Physiol* **274**:348-357 (1998).
21. Juan, S. H. *et al*. Tetramethylpyrazine protects rat renal tubular cell apoptosis induced by gentamicin. *Nephrol Dial Transplant* **22**:732-739 (2007).
22. Chen, Y. C. *et al*. Leptin reduces gentamicin-induced apoptosis in rat renal tubular cells via the PI3K-Akt signaling pathway. *Eur J Pharmacol* **658**:213-218 (2011).
23. Rovetta, F. *et al*. ER signaling regulation drives the switch between autophagy and apoptosis in NRK-52E cells exposed to cisplatin. *Exp Cell Res* **318**:238-250 (2012).
24. Renwick, L. C., Brown, D., Clouter, A. & Donaldson, K. Increased inflammation and altered macrophage chemotactic responses caused by two ultrafine particle types. *Occup Environ Med* **61**:442-447 (2004).
25. Grassian, V. H., O'shaughnessy, P. T., Adamcakova-Dodd, A., Pettibone, J. M. & Thorne, P. S. Inhalation exposure study of titanium dioxide nanoparticles with a primary particle size of 2 to 5 nm. *Environ Health Perspect* **115**:397-402 (2007).
26. De Jong, W. H. *et al*. Particle size-dependent organ

distribution of gold nanoparticle after intravenous administration. *Biomaterials* **29**:1912-1919 (2008).
27. Warheit, D. B. *et al*. Pulmonary toxicity study in rats with three forms of ultrafine-TiO_2 particles: differential responses related to surface properties. *Toxicology* **230**:90-104 (2007).
28. Asgharian, B. *et al*. Computational modeling of nanoscale and microscale particle deposition, retention and dosimetry in the mouse respiratory tract. *Inhal Toxicol* **26**:829-842 (2014).
29. Baggs, R. B., Ferin, J. & Oberdorster, G. Regression of pulmonary lesions produced by inhaled titanium dioxide in rats. *Vet Pathol* **34**:592-597 (1997).
30. Barillet, S. *et al*. Toxicological consequences of TiO_2, SiC nanoparticles and multi-walled carbon nanotubes exposure in several mammalian cell types: an in vitro study. *J Nanopart Res* **12**:61-73 (2010).
31. Tucci, P. *et al*. Metabolic effects of TiO_2 nanoparticles, a common component of sunscreens and cosmetics, on human keratinocytes. *Cell Death Dis* **4**:e549. doi: 10.1038/cddis.2013.76 (2013).
32. L'azou, B. *et al*. In vitro effects of nanoparticles on renal cells. *Part Fibre Toxicol* **5**:22 (2008).
33. Pan, Z. *et al*. Adverse effects of titanium dioxide nanoparticles on human dermal fibroblasts and how to protect cells. *Small* **5**:511-520 (2009).
34. Kansara, K. *et al*. TiO_2 nanoparticles induce DNA double strand breaks and cell cycle arrest in human alveolar cells. *Environ Mol Mutagen* **56**:204-217 (2015).
35. Botelho, M. C. *et al*. Effects of titanium dioxide nanoparticles in human gastric epithelial cells in vitro. *Biomed Pharmacother* **68**:59-64 (2014).
36. Møller, P. *et al*. Role of oxidative damage in toxicity of particulates. *Free Radic Res* **44**:1-46 (2010).
37. Noursadeghi, M. *et al*. Quantitative imaging assay for NF-κB nuclear translocation in primary human macrophages. *J Immunol Methods* **329**:194-200 (2008).
38. Birbach, A. *et al*. Signaling molecules of the NF-kappa B pathway shuttle constitutively between cytoplasm and nucleus. *J Biol Chem* **277**:10842-10851 (2002).
39. Napetschnig, J. & Wu, H. Molecular basis of NF-κB signaling. *Annu Rev Biophys* **42**:443-468 (2013).
40. Baldwin, A. S. Jr. The NF-kappa B and I kappa B proteins: new discoveries and insights. *Annu Rev Immunol* **14**:649-683 (1996).
41. Ding, G. J. *et al*. Characterization and Quantitation of NF-κB Nuclear Translocation Induced by Interleukin-1α and Tumor Necrosis Factor-α. *J Biol Chem* **273**:28897-28905 (1998).
42. Jiménez, L. A. *et al*. PM(10)-exposed macrophages stimulate a proinflammatory response in lung epithelial cells via TNF-alpha. *Am J Physiol Lung Cell Mol Physiol* **282**:L237-248 (2000).
43. Dianzani, M. U. Lipid peroxidation and cancer. *Crit Rev Oncol Hematol* **15**: 125-147 (1993).
44. Barrera, G. *et al*. 4-hydroxynonenal specifically inhibits c-myb but does not affect c-fos expressions in HL-60 cells. *Biochem Biophys Res Commun* **227**:589-593 (1996).
45. Barrera, G. *et al*. Effects of 4-hydroxynonenal, a product of lipid peroxidation, on cell proliferation and ornithine decarboxylase activity. *Free Radic Res Commun* **14**:81-89 (1991).
46. Raza, H. & John, A. 4-hydroxynonenal induces mitochondrial oxidative stress, apoptosis and expression of glutathione S-transferase A4-4 and cytochrome P450 2E1 in PC12 cells. *Toxicol Appl Pharmacol* **216**:309-318 (2006).